

Volatiles (S-CO₂-H₂O-Cl-F) Behavior during the AD 1944 Eruption

Angelo Paone

Department of Earth Sciences, University of Bristol, Bristol, UK
Email: angelo.paone1@gmail.com

Received 18 February 2015; accepted 14 March 2015; published 20 March 2015

Copyright © 2015 by author and Scientific Research Publishing Inc.
This work is licensed under the Creative Commons Attribution International License (CC BY).
<http://creativecommons.org/licenses/by/4.0/>



Open Access

Abstract

The AD 1944 is the last vulcanian-effusive eruption of Vesuvius volcano. I have reviewed most of the major and volatile elements in order to better understand the eruptive dynamic of this hazardous volcano. These volcanic products were basically formed by at least two main petrogenetic mechanisms: 1) mixing, 2) crystal fractionation. Crystal fractionation plays a major role in the evolution of the volcanic products of the AD 1944 eruption. According to the major elements data, several fractionation lines can be employed. Volatile data are analyzed in sequence. Indeed, the volatile data allow an insight into the exsolution and degassing processes occur during the growth and eruption of the AD 1944 eruption. Some inferences are also made on the exsolution and degassing depth. The volatile data illustrate a sequential order of exsolution for the AD 1944 eruption: Cl-H₂O-CO₂-S and finally as volatile phase degassed fluorine. The eruption has not interacted with external water. An early exsolution of Cl in Cl-rich magmas is also confirmed by experimental and geological studies (3 - 4 Kbars) coinciding with the deep magma reservoir.

Keywords

AD 1944 Eruption, Vesuvius, Degassing, Volatiles, Differentiation, Solubility

1. Introduction

On the scale of an individual eruption, volatiles affect nearly all aspects of its physical and chemical behavior. For example, volatiles affect solidus temperature, extent of melting; melt viscosity and thermodynamic properties, and finally eruption style.

Hence, understanding volatiles behavior on a single volcano will be crucial for evaluating and characterizing the volcanic hazardous. One important question is that when the single species (e.g., H₂O, CO₂, etc.) start to nucleate and when the bubble growth becomes interconnected, a viable way is made to escape. On other hand,

which is the depth single species starting to degas? It is known that volatiles generally decrease because the solubilities of the gas species (e.g., H_2O , CO_2 etc.) decrease with decreasing pressure.

The question is at which P-T condition and composition the magma get saturated of such species? How will the volatile species behave after that? This entire question can be applied to a single eruption. One eruption to be considered for reasons linked to the volcanic forecasting and hazard is the last eruption of Vesuvius volcano (AD 1944). To understand volatile behavior of this eruption is vital to understand the eruptive mechanism.

Petrogenetic Mechanism at the 1944 Eruption of Vesuvius by Melt Inclusion and Whole Rock Data

The major elements data on the 1944 eruption have been collected by several sources [1]-[6]. Variation diagrams have been made (*i.e.*, $\text{Al}_2\text{O}_3\text{-SiO}_2$, MgO-SiO_2 and CaO-SiO_2). CaO-SiO_2 diagram is shown to explain the petrogenetic mechanism during the 1944 last eruption of Vesuvius volcano relating the data on the lavas, scoria, and tephra and melt inclusion trapped into the main phenocrysts of respectively lava and tephra [3] [4]. The major element data (CaO-SiO_2 diagram, **Figure 1**) show that the melt inclusion trapped in the cpx of the 1944 lava flow has relatively more evolved composition in comparison with the lava whole rock data. This shift of the whole rock data at less evolved composition can be explained by mixing the composition of the lava melt inclusion with the melt inclusion trapped in the main phenocryst composing the tephra erupted successively (lava fountains and vulcanian phase, [4]). The bulk rock data of the pyroclastic products of the 1944 show that the melt evolves through mixing with a new magma batch which brings the composition to higher values of CaO and SiO_2 , to then evolve gradually through fractional crystallization to lower CaO values coinciding with the fractional crystallization evolutionary line of the broad 1944 volcanic products. The Alkali- SiO_2 (wt%) diagram is also shown (**Figure 2**). Features shown by this diagram follow the lines of reasoning of CaO-SiO_2 diagram. Finally, I can employ multi fractional crystallization evolutionary lines for the single 1944 AD eruption (**Figure 1**).

2. Sulfur Data

S data (**Figure 3**) are plotted against SiO_2 content [1] [3] [4] [7]. The melt inclusions trapped in the cpx of the 1944 lava flow eruption have a range that goes from 0.04 - 0.35 ppm. The bulk rock of the 1944 lava flow eruption have S content which reaches the lowest content at exactly 0.01 - 0.02. The 1944 scoria data from [4] give S values overlapping with the S bulk rock data. However, the melt inclusion trapped into the phenocrysts (cpx and

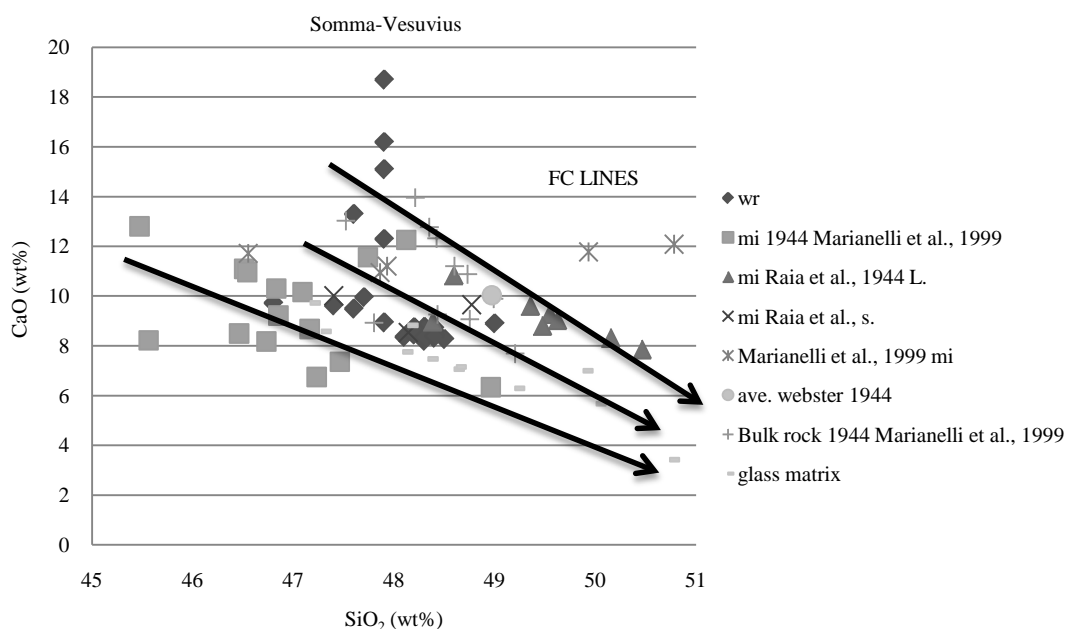


Figure 1. CaO-SiO_2 diagram.

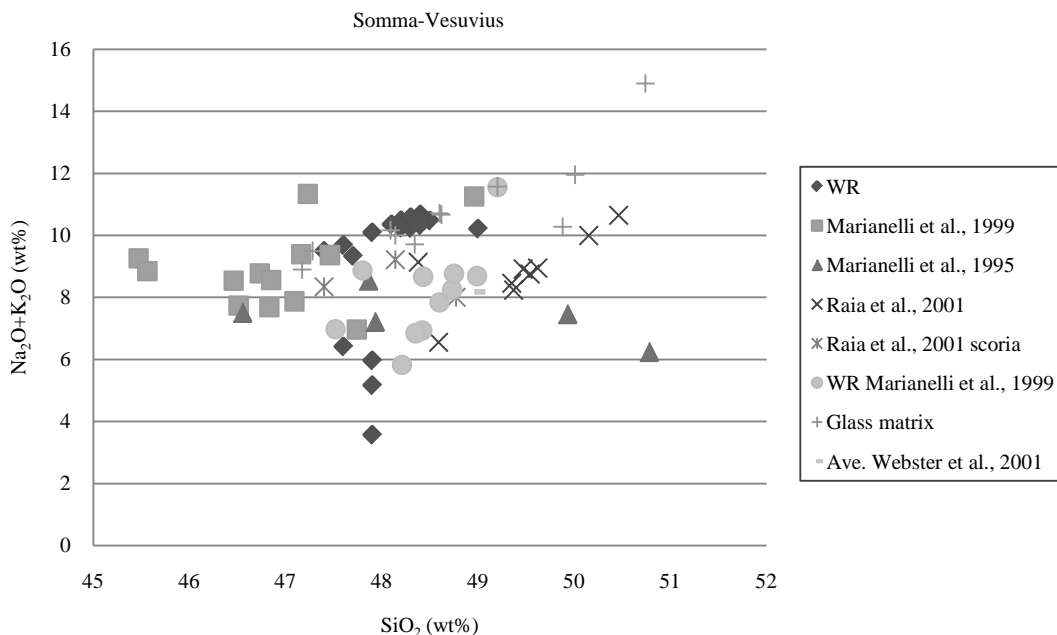


Figure 2. Alkali-SiO₂ diagram.

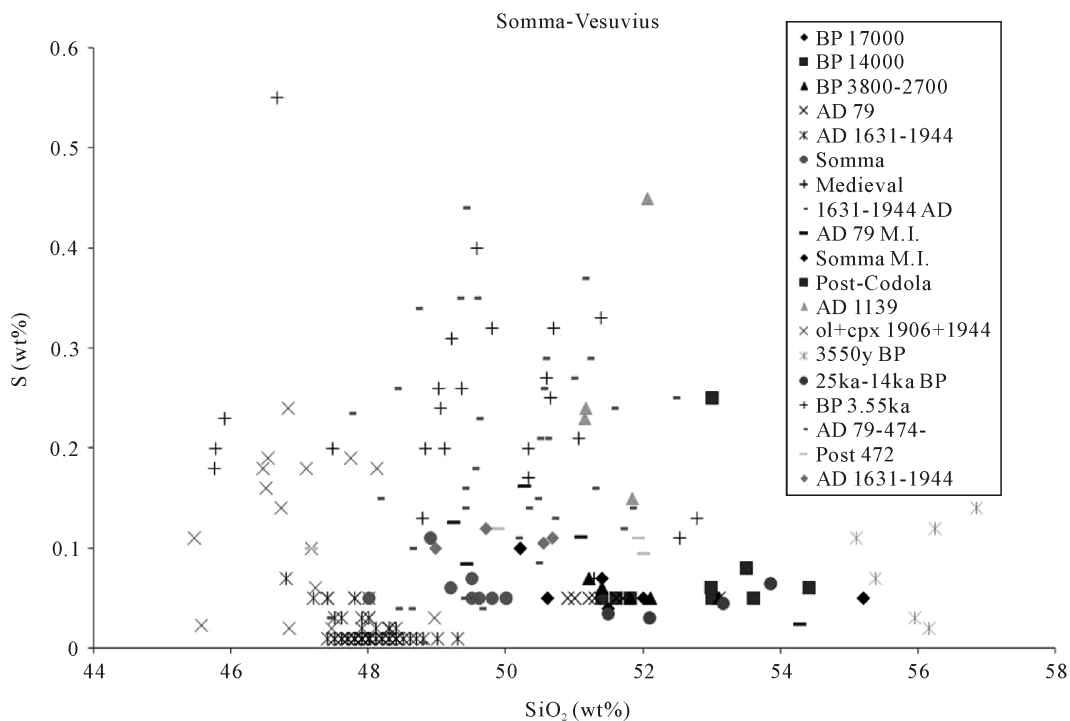


Figure 3. S-SiO₂ diagram.

ol) of the subsequently explosive activity of the 1944 Vesuvius activity (lava fountain and vulcanian phase) have higher values (S: 0.19 - 0.43).

This range of S data can be explained with a degassing syn-eruptive process which explains the decrease of S content from the melt inclusion trapped into the cpx in the lava to the S bulk rock. However, the fact that the melt inclusions trapped into the cpx and olivine of the subsequently explosive phases has higher S content has to be justified with the fact that probably the magma was not yet fully degassed.

3. Carbon Dioxide and Water Data

CO₂ data (Figure 4) are plotted against the SiO₂ content [1] [3] [4] [7]. Similarly, the features shown by the S-SiO₂ diagram are confirmed by the CO₂-SiO₂ diagram (Figure 2). Hence, the CO₂ data can be interpreted invoking the same degassing process as to explain the S degassing process.

CO₂ solubility in phonolite melt has been investigated by [8] and varies in function of the pressure and temperature (see Figure 4 in [8]). If the lower pressure experiment is taken (1.0 GPa) for comparison, the CO₂ solubility is nearly constant in function of the temperature (1300°C to 1600°C) at around 0.8 wt% CO₂. The broad CO₂ melt inclusion data have composition lower than the solubility limit of 1.0 GPa. CO₂ dissolved into the melt trapped into the ol, cpx of the final explosive phase of 1944 eruption have composition lower probably recording a lower depth of 1 GPa of origin which should suggest a lower CO₂ solubility limit at lower pressure following the [8] solubility data. This implies that probably the CO₂-saturation has been reached anyhow at lower pressure. [3] indicated an exsolution depth of 17 - 20 km.

Further, on the fluid inclusion studies [9] [10] show that the CO₂ and H₂O-CO₂ fluid inclusions are trapped on a depth range from 12 to 4 km. Although this data are not from the Vesuvius period, they suggest that broadly the CO₂ exsolve on this range of composition.

H₂O data (Figure 5) collected from the literature [1]-[3] [6] [7] plotted against the SiO₂ content show features similar to the S and CO₂ content against the SiO₂ content. These features are interpreted as S-CO₂-H₂O has behaved similarly during the 1944 eruption. Probably, the process to be invoked is the exsolution with this phases complexing together. However, the exsolution mainly was depended on the depth of the magma. The lower content of S-CO₂-H₂O in the melt inclusion of the lava flow products [4] is similar to the whole rock lava flow products which suggest that the degassing of this phases occurred before and during the eruption as testified by the crystallization of cpx in the 1944 lava probably in a shallow magma chamber. On the other hand, the higher content of the S-CO₂-H₂O on the melt inclusion of the last explosive period (strombolian and vulcanian phases) has changed the eruptive style. From the major element data, it is suggested that the magma batch of the explosive phase has a broad different composition from the composition of the first eruptive phase which implies that probably arrived in shallow magma chamber and mixed in a later time, following this line of reasoning, the volatile (S-CO₂-H₂O) confirm this hypothesis and suggest probably the later magma batch had increased the volatile (S-CO₂-H₂O) content by second boiling (crystallization processes).

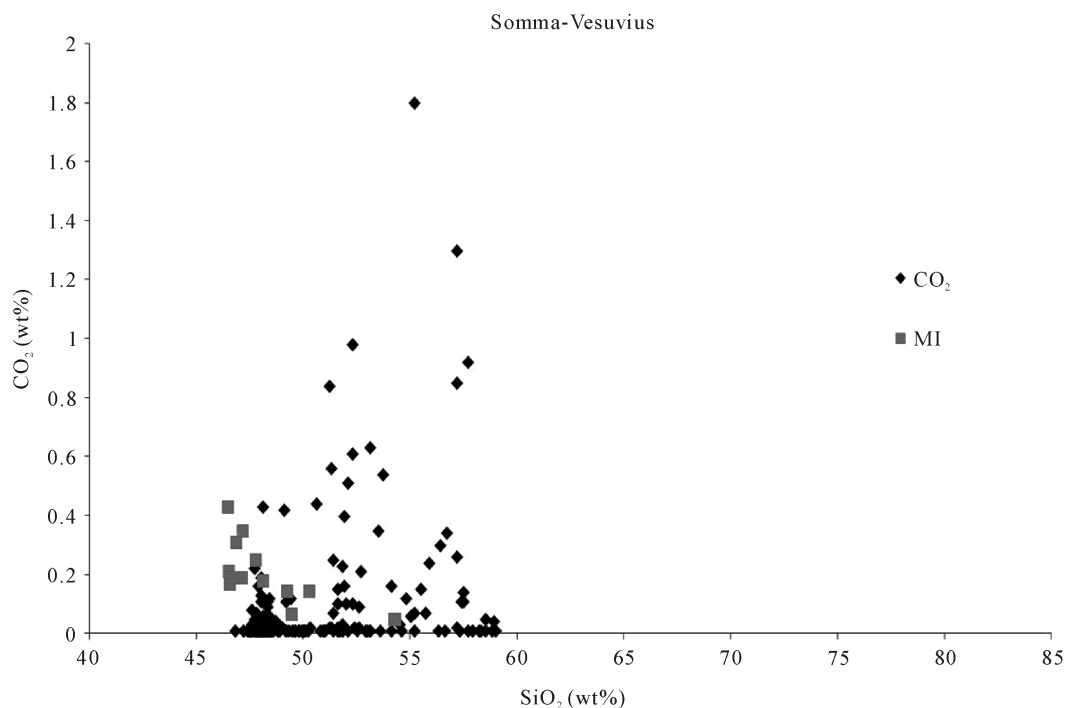


Figure 4. CO₂-SiO₂ diagram.

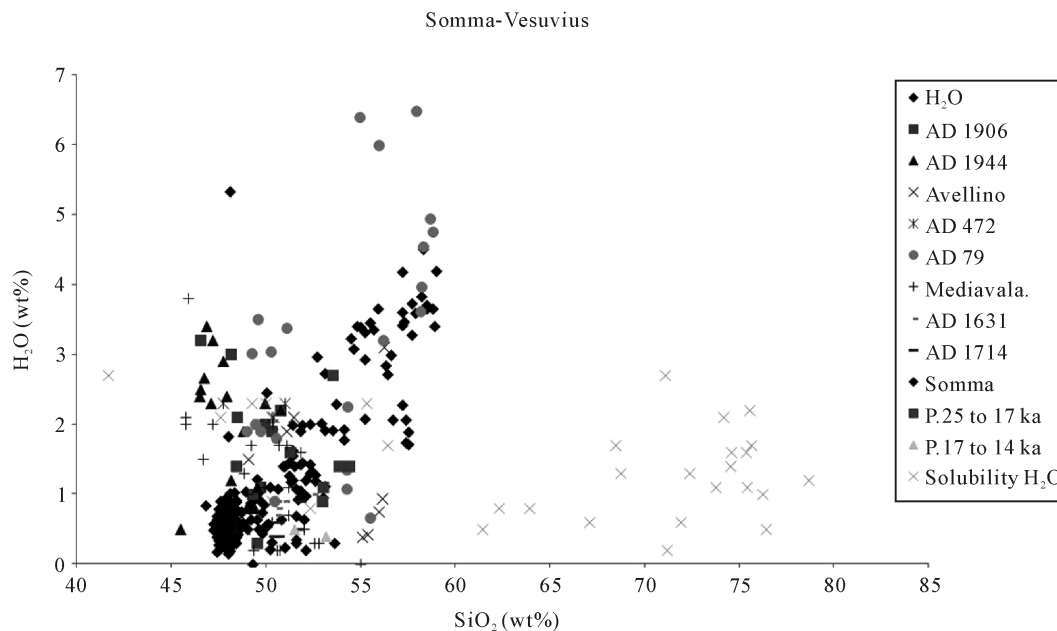


Figure 5. H₂O-SiO₂ diagram.

4. Chlorine Data

Cl data (**Figure 6(a)**) [1] [3] [4] [6] [7] show that the melt inclusion trapped inside the cpx of the lava flow and the main phenocrystals of the explosive activity of the 1944 eruption have flat trend (0.4 - 0.6 wt% Cl) against the SiO₂ (45 - 51 wt%). This trend is higher than Cl whole rock composition of the 1944 lava flow. From this data, the chlorine have degassed during the eruption. The nearly flat trend of Cl data suggest that the Cl has not participated into the built-up of explosive eruption which means that Cl have not increased into the melt by fractional crystallization processes to be then saturated and exsolve as volatile phases. Further, the fact that one melt inclusion of the 1944 tephra have a value of Cl content up to 1.28 wt% means that part of the melt trapped by minerals during the last explosive eruption dissolved very high Cl concentrations near the saturation value ([11], see also 12; references therein). The difference between the melt trapped at 1.28 wt% and the near flat trend between approximately 0.4 - 0.6 wt% Cl has to be explained with the exsolution of the Cl phases during the magma rise probably from 20 - 30 km. In fact, chlorine experimental work ([12], references therein) show that Cl solubility increase with magma decompression which further suggest an early exsolution of the chlorine. The flat trend is explainable with buffering the Cl by vapour phase which exsolve and complex with H₂O at lower depth [12]-[14]. The slight decrease along the differentiation (SiO₂: 45 - 50 wt%) can be accounted to the minor effect of crystallization Cl-bearing phases which are not prevalent in the 1944 Vesuvius magma. The Cl-H₂O solubility curves at 0.5 and 2 kbar are from the experimental data of [15] for haplogranite liquids at 800°C - 860°C. They suggest a trapping pressure ~2 kbar. Vapor plus hydrosaline liquid exsolve at the point of intersection; that is, the sharp break in the slope of the curves (e.g., [16]). The flat line shown by the Cl-H₂O data from trachyte-tephrite-phonolite of Somma-Vesuvius surely point to vapor plus hydrosaline liquid to exsolve at pressure higher than 3 - 4 kbars (**Figure 6(b)**).

5. Fluorine Data

Fluorine data are [1] [4] plotted against the SiO₂ content (wt%, **Figure 7**) for the AD 1944 eruption of Vesuvius. The F content of the melt inclusion trapped inside cpx of the lava and scoriae of the 1944 lava flow describe a flat trend, slightly increasing (0.33 - 0.41) versus the differentiation index (SiO₂: 47.4 wt% - 50.15 wt%). The slight increase has due to the >1 bulk distribution coefficient in the AD 1944 melt. The fluorine relationship between the whole rock and melt inclusion data show that the whole rock has a lower F content (0.11 wt% - 0.29 wt%) compared to the melt inclusion. However, some melt inclusion data overlap the range of fluorine whole rock data. The difference in fluorine content suggests that during the lava flow eruption, fluorine degassing has

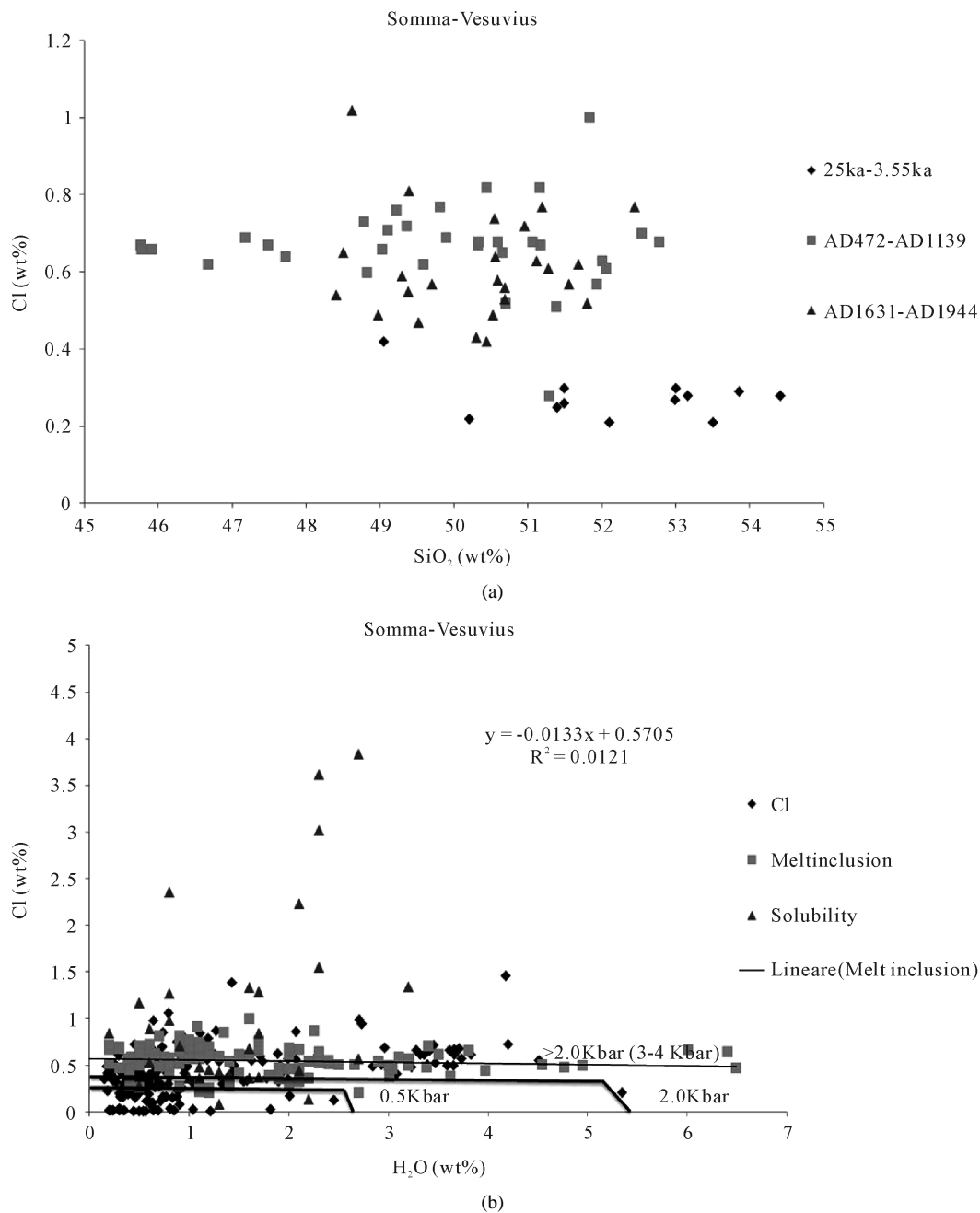


Figure 6. (a) Cl-SiO₂ diagram; (b) Cl-H₂O diagram.

occurred. Probably, the F melt inclusion data also suggest that fluorine started to degas early on during the crystallization of cpx inside the melt that produced the AD 1944 lava flow as testified by some melt inclusion with low fluorine content overlapping the F whole rock data.

6. Discussion and Conclusions

From the bulk of major elements and volatile data recovered from the literature [1]-[6], it is possible to draw a schematic behavior of the AD 1944 eruption. The major element data illustrate the petrogenetic mechanism of the AD 1944 eruption. These volcanic products are basically formed by at least two main petrogenetic mechanisms: 1) mixing, 2) crystal fractionation. The melt inclusion data record at least two mixing events occurs

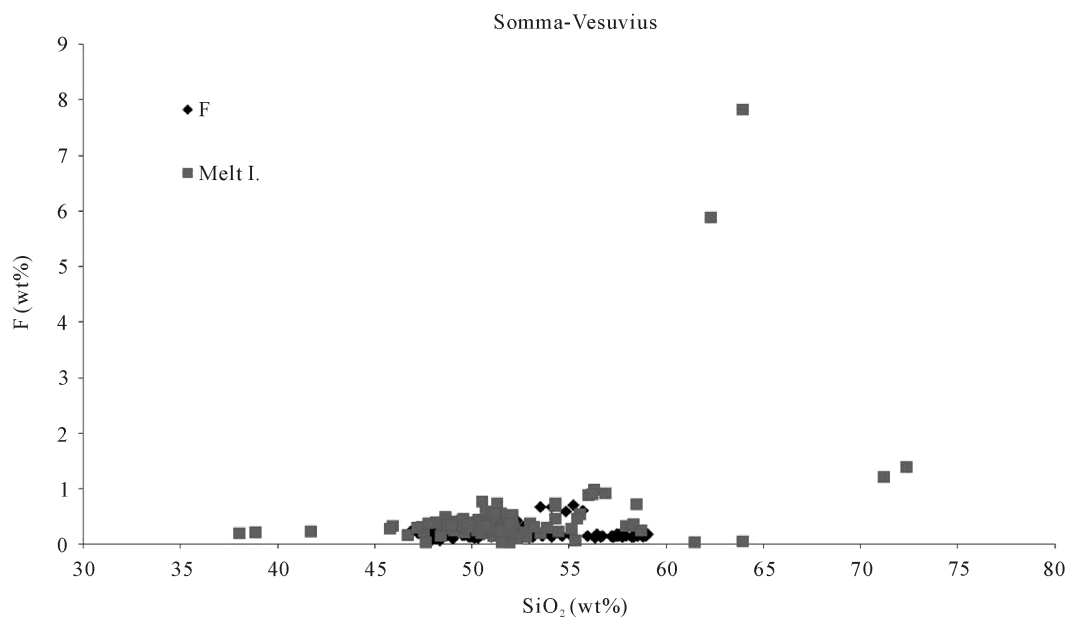


Figure 7. F-SiO₂ diagram.

during the growth of the magma chamber of the AD 1944 eruption. Crystal fractionation has worked all along the time of growth of the AD 1944 magma chamber as testified by the volcanic products.

The volatile data (S-CO₂-H₂O-Cl-F) broadly confirm the petrogenetic schematic scheme drawn by major element data. Furthermore, the volatile data allow an insight into the exsolution and degassing processes occurred during the growth and eruption of the AD 1944 eruption. Some inferences are also made on the exsolution and degassing depth. The volatile data illustrate a sequential order of exsolution for the AD 1944 eruption: Cl-H₂O-CO₂-S and finally as volatile phase degassed fluorine. An early exsolution of Cl in Cl-rich magmas is also confirmed by experimental and geological studies [12]. The inferred beginning of chlorine depth of exsolution for the AD 1944 magma is hypothesized to be as start the magma formation between 20 - 30 km [17] which should be also the shallow magmatic depth of origin. During the magma rise, the chlorine is buffered by a vapour-phase (maybe H₂O-CO₂) which stabilizes the chlorine content in the melt between 0.4 wt% - 0.6 wt%. The fact that H₂O-CO₂-S behaves similarly in the AD 1944 magma should suggest that probably the fluid phase that buffers chlorine is a complexing form by H₂O-CO₂-S volatile phases. Probably, the main gases phases candidate for the beginning of fractionation in the magma chamber is H₂O-CO₂-S, in fact the last explosive phases versus the lava flow activity are enriched of this phases. The interaction of the AD 1944 magma with some external source (*i.e.*, aquifer) is discarded by the volatile data. Fluorine does not participate in any exsolution process. The bulk volatile data confirm a wide syn-eruptive degassing of (S-H₂O-CO₂-Cl-F) especially during the AD 1944 eruption.

Acknowledgements

This work is initiated at University of Bristol with Marie Curie Fellowship (individual post-doc, 2001-2003). Thanks to Chris Hawkesworth to host me and to be my tutor. The work has been pending for more than 10 years, and now I have decided to finalize my idea.

References

- [1] Belkin, H.E., Kilburn, C.R.J. and De Vivo, B. (1993) Chemistry of the Lavas and Tephra from Recent (AD 1631-1944) Vesuvius (Italy) Volcanic Activity. US Geological Survey Open-File Report 93-399, 44.
- [2] Marianelli, P., Metrich, N., Santacroce, R. and Sbrana, A. (1995) Mafic Magma Batches at Vesuvius: A Glass Inclusion Approach to the Modalities of Feeding Stratovolcanoes. *Contributions to Mineralogy and Petrology*, **120**, 159-169. <http://dx.doi.org/10.1007/BF00287113>
- [3] Marianelli, P., Metrich, N. and Sbrana, A. (1999) Shallow and Deep Reservoirs Involved in Magma Supply of the 1944

- Eruption of Vesuvius. *Bulletin of Volcanology*, **61**, 48-63. <http://dx.doi.org/10.1007/s004450050262>
- [4] Raia, F., Webster, J.D. and De Vivo, B. (2000) Pre-Eruptive Volatile Contents of Vesuvius Magmas: Constraints on Eruptive History and Behavior. I. The Medieval and Modern Interplinian Activities. *European Journal of Mineralogy*, **12**, 179-193. <http://dx.doi.org/10.1127/0935-1221/2000/0012-0179>
- [5] Fulignati, P., Marianelli, P. and Sbrana, A. (2000) Glass-Bearing Felsic Nodules from the Crystallizing Sidewalls of the 1944 Vesuvius Magma Chamber. *Mineralogical Magazine*, **64**, 481-496. <http://dx.doi.org/10.1180/002646100549373>
- [6] Webster, J.D., Raia, F., De Vivo, B. and Rolandi, G. (2001) The Behavior of Chlorine and Sulfur during Differentiation of the Mt. Somma-Vesuvius Magmatic System. *Mineralogy and Petrology*, **73**, 177-200. <http://dx.doi.org/10.1007/s007100170016>
- [7] Ayuso, R.A., De Vivo, B., Rolandi, G., Seal, R.R. II and Paone, A. (1998) Geochemical and Isotopic (Nd-Pb-Sr-O) Variations Bearing on the Genesis of Volcanic Rocks from Vesuvius, Italy. *Journal of Volcanology and Geothermal Research*, **82**, 53-78. [http://dx.doi.org/10.1016/S0377-0273\(97\)00057-7](http://dx.doi.org/10.1016/S0377-0273(97)00057-7)
- [8] Morizet, Y., Brooker, R.A. and Kohn, S.C. (2002) CO₂ in Haplo-Phonolite Melt: Solubility, Speciation and Carbonate Complexation. *Geochimica et Cosmochimica Acta*, **66**, 1809-1820. [http://dx.doi.org/10.1016/S0016-7037\(01\)00893-6](http://dx.doi.org/10.1016/S0016-7037(01)00893-6)
- [9] Belkin, H.E., De Vivo, B., Roedder, E. and Cortini, M. (1985) Fluid Inclusion Geobarometry from Ejected Mt. Somma-Vesuvius Nodules. *American Mineralogist*, **70**, 288-303.
- [10] Belkin, H.E. and De Vivo, B. (1993) Fluid Inclusion Studies of Ejected Nodules from Plinian Eruptions of Mt. Somma-Vesuvius. *Journal of Volcanology and Geothermal Research*, **58**, 89-100. [http://dx.doi.org/10.1016/0377-0273\(93\)90103-X](http://dx.doi.org/10.1016/0377-0273(93)90103-X)
- [11] Paone, A., Webster, J., Raia, F. and De Vivo, B. (2001) Preliminary Results of Melt Inclusion and Experimental Volatile Solubility Studies for Alkaline Magmas of Mt. Somma-Vesuvius Volcano. EGS 2001 Abstract.
- [12] Webster, J.D. and De Vivo, B. (2002) Experimental and Modeled Solubilities of Chlorine in Aluminosilicate Melts, Consequences of Magma Evolution, and Implications for Exsolution of Hydrous Chlorine Melt at Mt. Somma-Vesuvius. *American Mineralogist*, **87**, 1046-1061.
- [13] Signorelli, S. and Capaccioni, B. (1999) Behavior of Chlorine Prior and during the 79 AD Plinian Eruption of Vesuvius (Southern Italy) as Inferred from the Present Distribution in Glassy Mesostases and Whole-Pumices. *Lithos*, **46**, 715-730. [http://dx.doi.org/10.1016/S0024-4937\(98\)00092-9](http://dx.doi.org/10.1016/S0024-4937(98)00092-9)
- [14] Webster, J.D., Kinzler, R.J. and Mathez, E.A. (1999) Chlorine and Water Solubility in Basalt and Andesite Melts and Implications for Magma Degassing. *Geochimica et Cosmochimica Acta*, **63**, 729-738. [http://dx.doi.org/10.1016/S0016-7037\(99\)00043-5](http://dx.doi.org/10.1016/S0016-7037(99)00043-5)
- [15] Webster, J.D. (1997) Exsolution of Magmatic Volatile Phases from Cl-Enriched Mineralizing Granitic Magmas and Implications for Ore Metal Transport. *Geochimica et Cosmochimica Acta*, **61**, 1017-1029. [http://dx.doi.org/10.1016/S0016-7037\(96\)00395-X](http://dx.doi.org/10.1016/S0016-7037(96)00395-X)
- [16] Webster, J.D. (2004) The Exsolution of Magmatic Hydrosaline Chloride Liquids. *Chemical Geology*, **210**, 33-48. <http://dx.doi.org/10.1016/j.chemgeo.2004.06.003>
- [17] De Natale, G., Troise, C., Pingue, F., De Gori, P. and Chiarabba, C. (2001) Structure and Dynamics of the Somma-Vesuvius Volcanic Complex. *Mineralogy and Petrology*, **73**, 5-22. <http://dx.doi.org/10.1007/s007100170007>